POPULATION GENETIC STRUCTURE OF UNIONID MUSSELS ACROSS MULTIPLE GULF DRAINAGES

by

Matthew Stewart Harrison, BS

A thesis submitted to the Graduate Council of
Texas State University in partial fulfillment
of the requirements for the degree of
Master of Science
with a Major Population and Conservation Biology
December 2022

Committee Members:

Noland H. Martin, Chair

Chris Nice

Timothy Bonner

FAIR USE AND AUTHOR'S PERMISSION STATEMENT

Fair Use

Duplication Permission

ACKNOWLEDGEMENTS

I would like to first thank my thesis committee for the endless patience, advice, and support given to me during my time as a Master's student. I gratefully acknowledge the funding received for this project from the Texas State University Biology Department, and the Sabine River Authority. I would like to thank the members of the Nice, Ott, Martin, and Bonner labs for all the help in completing this project. I'd also like to thank Brad Littrell and Biowest crew, the Sabine River Authority, the Lower Neches Valley Authority, and Chase Smith for aid in procuring samples. Finally, I would like to thank several others including Avery Mottet, Alex Guzman, Alex Sotola, and Alex Zalmat for endless support and aid in lab work and computing.

TABLE OF CONTENTS

Page

LIST OF TABLES

Table **Page**

LIST OF FIGURES

Figure **Page**

ABSTRACT

Understanding patterns of genetic differentiation within and across wildlife populations is a key component to parsing the demographic and ecological processes that govern the spatial structure and evolutionary trends of a given species. As molecular and computational techniques continue to advance, these data have become critical tools in delineating population boundaries as well as informing appropriate management decisions. This study utilized a genotyping by sequencing (GBS) approach to study the genetic structure of three Texas state threatened mussel species of family Unionidae: *Pleurobema riddellii* (Louisiana Pigtoe), *Fusconaia askewi* (Texas Pigtoe), and *Potamilus amphichaenus* (Texas Heelsplitter). Principal component and admixture analyses paired with genetic distance estimates (G_{ST}) of these species demonstrated clear interspecific and intraspecific differentiation across separate drainages as well as indications of isolation within drainages potentially facilitated by geographic barriers such as river impoundments and local environmental and ecological differences. These data present an effective approach to modeling genetic structure across a landscape that allow for precise inferences on population boundaries that inform conservation units (CU's) and the management strategies that use them (Funk et al., 2012; Smith et al., 2021).

I. INTRODUCTION

Isolation amongst fragmented populations serves as a major component to genetic differentiation within species and can potentially have a number of associated demographic and evolutionary consequences including differential genetic drift, divergence, loss of genetic variability, and local extinction (Templeton et al., 1990; Hanski et al., 1995). Additionally, differentiation due to geographic isolation may be further compounded by secondary contact and reinforcement that generates selection against divergent ecological, behavioral, or morphological lineages (Bush, 1969; Bolnick & Fitzpatrick, 2007). Physical and geographical barriers remain an important factor in the reduction of gene flow between populations (Steeves et al., 2003; Trizio et al., 2005; Riley et al., 2006; Zalewski et al., 2009) and can have a number of long- and short-term evolutionary effects on within-population genetic variation and between-population genetic divergence resulting from factors such as different dispersal capabilities and varying affinities for environmental conditions (Spieth, 1974; Spieth 1979). Modern population fragmentation is further exacerbated by ongoing human encroachment, often manifesting as the alteration and disruption of natural habitat, as well as the construction of artificial barriers. In this study, we investigate the extent of genetic differentiation and its spatial patterning among freshwater mussels in order to better delineate population boundaries and their potential causes.

Understanding the distribution of genomic variation of species subject to these recent and historical habitat changes is key to assessing the potential risks faced by certain populations and potential conservation strategies to ameliorate them. The linear flow of rivers, having an inherent effect on patterns of dispersal and gene-flow, not only

creates a unique framework in which to study patterns of genetic exchange within and between watersheds, but also presents a suite of distinct concerns for conservation efforts such as historical connectivity of rivers and drainages, and the construction of impoundments altering environmental conditions as well as serving as physical barriers between populations (Randklev et al., 2011; Schaefer et al., 2011).

Bivalves of order Unionoida (freshwater mussels) occupy a nearly worldwide distribution, inhabiting freshwater lakes and rivers within six of the seven continents (excluding Antarctica). The North American continent boasts the majority of *Unionid* diversity - comprising approximately a third of its described species (~297 spp.) (Ricciardi et al., 1998; Lydeard et al., 2004). Despite this diversity, unionid mussels are considered one of the most imperiled groups within North America with approximately 12% (35 spp.) presumed extinct and ~60% facing some form of threat often attributed to environmental degradation in the form of pollution, impoundment, and newly introduced species such as the Eurasian Zebra Mussel (*Dreissena polymorpha*) (Williams et al., 1993; Lydeard et al., 2004; Archambault et al., 2014; Olson & Vaughn, 2020). The spatial distribution of unionid mussel populations consists primarily of dense beds of sedentary adults acting as sub-populations separated by mostly depauperate stretches of river (Strayer et al., 2004; Olson & Vaughn, 2020), with the mussel glochidia larvae, obligate ectoparasites of fish, providing the most mobility throughout the lifecycle of an individual mussel (Barnhart et al., 2008). The combination of these factors results in the majority of gene-flow among populations likely being limited to movement of dispersal via host fish, or downstream flow of sperm, juvenile mussels, or glochidia lacking a host (Schwalb et al., 2011; Ferguson et al., 2013; Irmscher & Vaughn, 2018). Unraveling the

genetic connectivity of these populations will be essential in diagnosing isolation among disparate populations and prescribing appropriate management solutions - especially in the context of recent and future habitat alteration.

Unionids represent a relevant and effective model organism to study in the context of fresh-water population demographics. This study focused on population genetic structure of three Unionid species: *Pleurobema riddellii* (Louisiana Pigtoe), *Fusconaia askewi* (Texas Pigtoe), and *Potamilus amphichaenus* (Texas Heelsplitter), all of which are currently listed as threatened in the State of Texas (TPWD, 2020). The study was largely confined within the Neches, Sabine, and Mississippi drainages of the United States gulf coast and utilizes a genotyping by sequencing (GBS) approach to: 1) confirm the putative species designations provided by field-identifications of the three target taxa, 2) determine the degree to which population structure between the three drainages is consistent with an expectation of historical isolation and divergence, 3) characterize genetic structure within drainages and its correlation with isolation by distance or specific geographical or ecological phenomena, and 4) to assess similarities or differences in structural pattern across species that co-occur in the sampled drainages.

Answering these questions and identifying notable areas of differentiation may help identify specific physical features or unique environments that may be driving divergence and, in turn, provide vital resources in establishing the population units used in conservation and management strategies. I hypothesized that different species should appear genetically distinct using ordination techniques, which would thereby prove useful in the assessment of field identifications. When analyzed individually, I further

hypothesized that species should consistently reflect clear genetic delineation between separate drainages indicative of neutral divergence.

II. METHODS

-Collection of Samples

Sample tissue for *Pleurobema riddellii*, *Fusconaia askewi*, and *Potamilus amphichaenus* was collected across 27 total sites and three drainages (Neches, Sabine, and Mississippi). Mussels were collected by diving and grubbing by hand followed by identification by putative species using morphological traits. Once identified, tissue plugs were collected from each individual using a nasal biopsy tool before relocating back to their respective collection locations. Tissue samples were stored in 95% ethanol on dry ice before relocation to a -20°C freezer. Within this collection *P. riddellii* samples were represented in 21 sites across all three drainages (Table 2, Figure 1), *F. askewi* in seven sites across two drainages (Neches and Sabine)(Table 4, Figure 2), and *P. amphichaenus* in six sites across two drainages (Neches and Sabine)(Table 6, Figure 3). Three sites within the Neches basin were located on the Lower Neches Valley Authority (LNVA) canal.

-DNA generation, assembly, and filtering

DNA was extracted from mussel foot-tissue plugs representing 384 total individuals using the Qiagen DNeasy blood and tissue kit in 96-well format. Extracted DNA was used to create a reduced-complexity genomic library for each individual using modified protocols from (Gompert et al., 2012; Mandeville et al., 2015; Parchman et al., 2012; Sotola et al., 2018). Restriction enzymes EcoRI and MseI were used to digest sample DNA with EcoRI adapters on resulting fragments being ligated with 10-20 base pair multiplex identifier sequences (MIDs). Labeled products were amplified through two rounds of PCR using Illumina primers. PCR products were pooled into a single library

and sent to the University of Texas Genomic Sequencing and Analysis Facility (Austin, TX).

Bowtie v.3 was used to identify PhiX control sequences, with reads assembling to the PhiX genome being removed. Custom pearl scripts were used to match sample IDs with unique barcode identifiers and remove Mse1 adapters and barcodes from sequence reads. Sequence data was then organized into five assemblies for separate analyses. First, a "complete" (all sequenced individuals) assembly was filtered and analyzed using principal component analysis (PCA) to evaluate accuracy of field IDs as well as overall coverage of individuals. The other five assemblies were constructed separately for each sampled species. *Pleurobema riddellii* was investigated using two different assemblies of collected individuals: one containing all individuals that were collected within the species (total sampling effort), and another only using samples from the Neches and Sabine drainages of East Texas. This smaller assembly was included to provide an analysis that was directly comparable to the other species (both restricted to the Neches and Sabine drainages) as well as the possibility of identifying an increased number of assembly-wide genetic variable sites. Due to neutral divergence in restriction-site evolution, subsets of less differentiated populations may result in less missing data between individuals and therefore the retention of more SNPs. This may, in turn, provide increased resolution to identify lower-level structural patterns within this group.

In lieu of reference genomes for collected species, de novo assembly scaffolds were created using part of the dDocent pipeline (Puritz, Hollenbeck, & Gold, 2014). I removed reads with less than 4 copies per individual and shared among less than 4 individuals. Remaining reads were assembled with CD-hit (Fu et al., 2012; Li & Godzik,

2006) allowing up to 80% homology. Sequence reads were assembled to the de novo scaffolds using the aln and samse algorithms from BWA (version 0.7.13-r1126)(Li & Durbin, 2009). BCFtools (version 1.9)(Li, 2011) was used to both identify variable sites (Single Nucleotide Polymorphisms, hereafter SNP's) as well as calculate Bayesian posterior probabilities of variable individual SNP's. Loci must have been represented by at least 80% of the individuals (minimum of one read) in a given assembly in order to be included in the respective dataset. Additionally, a custom perl script was used to filter out low coverage SNPs, only retaining individuals with an average sequence depth of two reads per individual(mean sequence depth $\geq$ 2*n). This perl script was also used to remove potentially paralogous loci with exceptionally high sequence depth. These loci were defined as those with an average coverage exceeding the 95th percentile (mean sequence depth > assembly-wide mean + 2*sd). This script also filtered loci based on mapping quality (minimum of 30), as well as the difference in base and mapping quality between the reference and alternative alleles using the Mann-Whitney U test (z-score cutoff = 1.96). Genotype likelihoods were assigned to each SNP for each individual and used to calculate population allele frequencies; SNP's with a minor allele frequency of <0.05 were not included in the final data. One SNP per contig was chosen at random using custom perl scripts to reduce any effects of linkage disequilibrium. Additionally, individuals within assemblies with a mean coverage of <4 reads per locus were not included in final analyses.

-Population Genetic Structure

Genetic parameters were derived from Entropy (Gompert et al., 2014; Mandeville et al., 2015) a hierarchical model in which Bayesian-based admixture proportions and

genotype likelihoods are estimated for each individual among some predetermined number of populations (k). Genetic structure of each assembly was first inspected through a principal component analysis (PCA) using our genotype likelihoods. PCA results were used as a rough means of assessing the accuracy of field IDs in the "complete" assembly given that field identification of mussel can be subject to error without substantial experience (Howells et al., 2017). Models illustrating our admixture results for k= 2-4 (2-6 for *P.* riddellii) are included to provide as much context as possible when examining the hierarchical relationships between sampling regions. While results of this model (and their interpretation) are similar to those of Structure (Falush et al., 2003; Pritchard et al., 2000), Entropy differs from Structure in its accounting of genotyping errors, variation in sequence alignment and coverage, and production of posterior genotype probability distributions using prior probabilities of cluster allele frequencies (Gompert et al., 2014a; Sotola et al., 2018). Calculation of posterior distributions for each k was done using a Markov Chain Monte Carlo (MCMC) algorithm including 55,000 total iterations with a burn-in of 5,000 and sampling every 10^{th} iteration. The MCMC model for each k was run twice and averaged across both runs (genotype and admixture proportions) after checking chain convergence using Gelman-Rubin diagnostic statistics and effective sample sizes. Genetic distance between sampling sites was further inspected by calculating pairwise values of Nei's G_{ST}. Allele frequencies used for G_{ST} estimates were calculated using genotype likelihoods from Entropy in R (R Core Team, 2021).

III. RESULTS

-Field sampling

Sample size of individuals per species per collection site ranged from one to 27. Subsequent sequencing resulted in 485,754,716 raw reads with an average of 1,264,986 sequences per individual. Probable field misidentifications were identified in PCA as those whose field-identified species did not match with the respective species cluster in which they were located (Figure 4) and were excluded from subsequent analyses.

-Complete assembly

The complete assembly included data for 352 individuals across the three species analyzed here, as well as an additional two species: *Leptodea fragilis* and *Cyclonaias pustulosa*. This resulted in 3,621 SNP's (Table 1) each with an average of 13.71 (sd=5.36) reads per locus per individual. Principal component I explained 34.28% of the variation, and principal component two explained 22.56% of the variation (Figure 4). The PCA indicated six clusters comporting with the five sampled species in addition to a putative sixth species that comprised misidentified *P. riddellii*. This sixth species potentially represents the Wabash Pigtoe (*Fusconaia flava*) given its sample region and proximity to the *F. askewi* cluster. 20 individuals were strongly associated with clusters that did not match their associated field ID (*P. riddellii* = 12, *F. askewi* = 4, *C. pustulosa* = 4), and were not included in subsequent assemblies and analysis.

-Pleurobema riddellii

The assembly including all *P. riddellii* samples represented 147 individuals and 14,928 SNP's (Table 1) with an average of 5.61 (sd = 1.29) reads per locus per individual. Principal component I explained 5.75% of the variation while principal

components II and III explained 1.97% and 1.79% respectively. Comparing principal component I versus II produced three clusters: PC I separated the Texas drainages (Neches and Sabine Rivers) from the Little River and Big Cypress individuals with the Ouachita samples lying between. PC II primarily separated the Ouachita samples from all others. PC III separated the Neches and Sabine drainages into two separate clusters (Figure 5).

Entropy was used to calculate admixture proportions for k = 2-6 across the larger *P. riddellii* assembly (Figure 6). At k=2, the model reflected a pattern consistent with PC I, separating out the two Texas drainages from the Little River and Big Cypress Bayou samples while the Ouachita and Pearl samples showed intermediate admixture assignments. This pattern continued with k=3 separating out the Ouachita samples into their own cluster, and k=4 further separating the two Texas drainages into independent clusters. At k's 5-6, the model began to identify sub-structure within the Neches drainage grouping. G_{ST} estimates were largely consistent with this pattern, with both Little River and Ouachita River sites both displaying relatively high pairwise values (means of 0.150 and 0.098 respectively) when compared to sites within the Neches or Sabine drainages. Mississippi and Sabine drainage comparisons (mean = 0.131) and Mississippi and Neches comparisons (mean = 0.119) were only slightly higher than the Mississippi intra-drainage value (Little River and Ouachita River G_{ST} = 0.110), however all of these values indicate a much higher level of differentiation relative to Neches and Sabine site comparisons (mean = 0.047). Intra-drainage values for the Sabine and Neches were relatively lower (means = 0.058 & 0.027 respectively) and showed no significant substructure pattern with the exception of one Neches canal site showing consistently

high values when compared to other sites in the Neches drainage (mean = 0.050)(Table 3).

The additional assembly containing only samples from the Neches and Sabine drainages, represented 130 individuals and 14,955 SNP's (Table 1) with an average of 5.74 (sd=1.28) reads per locus per individual. This smaller group was analyzed hoping to gain a higher resolution of community structure due to the higher SNP count and coverage post-filtering, as well as to mirror the scope of analysis for the other species in this study. Principal components I and II explained 2.14% and 1.42% of the total variation respectively and revealed two major clusters that distinguished the two sampled drainages as well as some slight separation within the Neches drainage individuals (Figure 7).

Admixture proportions were calculated for k = 2-4 for the Texas *P. riddellii* samples (Figure 8). This model remained consistent with the corresponding PCA as well as the larger *P. riddellii* assembly results with k=2 effectively separating the Neches and Sabine drainages, and k's 3 and 4 resulting in substructure within the larger Neches sample group. There were no substantial differences in G_{ST} values in the smaller assembly.

-*Fusconaia askewi*

The assembly for *F. askewi* represented 96 individuals and 26,755 SNP's (Table 1) with an average of 4.95 (sd=1.10) reads per locus per individual. Principal component analysis revealed three primary clusters that separated individuals sampled from the Neches drainage, upper Sabine, and lower Sabine (Figure 9). Principal component I explained 3.52% of the total variation, this axis mostly separated the lower Sabine sample

group from the upper Sabine and Neches groups. Principal component II explained 2.52% of the total variation and showed relatively even spacing between clusters with the lower Sabine cluster falling between the Upper Sabine and Neches clusters.

Admixture proportions were calculated for k = 2-4 for *F. askewi* samples (Figure 10). At k=2 individuals from the Neches and upper Sabine clustered together while the lower Sabine individuals were in a cluster of their own. Samples from the lower Neches sample site (n=3) also showed slight admixture with the lower Sabine cluster. At k=3 the Neches samples were separated from the upper Sabine group, however the three individuals from the lower Neches site still showed admixture with the lower-Sabine group. Higher levels of k only revealed slight substructure within individuals collected from the upper Sabine group. High differentiation in the lower Sabine was also reinforced by the G_{ST} estimates, with lower-Sabine and upper-Sabine comparisons (mean = 0.051) higher than Neches and Sabine comparisons (0.045) as well as any intra-drainage value (Neches G_{ST} = 0.043; Sabine drainage mean = 0.037). This is even more striking when excluding the lower-Sabine from comparisons, lowering both the Neches and Sabine average (mean = 0.042) as well as the Neches intra-drainage value (G_{ST} = 0.028)(Table 5).

-*P. amphichaenus*

The *P. amphichaenus* assembly represent 28 sampled individuals and 21,020 SNP's (Table 1) with an average of 6.76 (sd=1.81) reads per locus per individual. Principal component analysis indicated two clusters separating individuals sampled from the Neches and Sabine drainages. Principal component I explained 5.24% of the variation and is the primary axis separating the two clusters (Figure 11). Principle components II,

III, and IV explained 4.56, 4.36, and 3.94% respectively and only revealed variation within each of the two primary clusters.

Admixture proportions for k = 2 revealed two primary clusters between the Neches and Sabine drainages with no evidence of admixture. At k = 2 and 3, slight substructure was revealed within the Neches samples (Figure 12). G_{ST} estimates between Neches and Sabine samples remained consistent with previously mentioned species (G_{ST} = 0.043) (Table 7).

IV. DISCUSSION

Better understanding of genetic structure and gene flow can help inform strategies that may be used for protection and recovery plans for imperiled mussel taxa, and with modern technology and techniques allowing for powerful genetic analyses using GBS data, it's possible to probe population structure of non-model species of interest that may be indicative of isolation and divergence. Given fluctuations in the biotic and abiotic environment of watersheds associated with modern processes such as climate change, habitat alteration, and land use (Cañeda-Argüelles et al., 2013; Phillips et al., 2004; Randklev et al., Wellmeyer et al., 2005), the formation of mitigation and recovery strategies that can properly address unique populations is crucial.

Analyses utilizing genome-wide markers allow for the drawing of inferences about patterns of genetic structure and gene flow through the formation of clusters at multiple levels of resolution, thus allowing a more comprehensive perspective of population demographics within a given region. Given the geographically determined limitations that are inherent to any linear riverine system, null expectations for population genetic structure in these systems would primarily be based on a model of isolation by distance whereby intra-drainage structure is dictated by stream-order and environmental gradients (Vannote et al., 1980) while inter-drainage patterns correspond to historical and contemporary drainage proximity consistent with processes of allopatric divergence. Sequence data here has shown to be largely consistent with the expectation of drainage delineation with clear differentiation between watersheds. No correlative analysis was included examining river-distance and differentiation (G_{ST}) within drainages, however comparisons between the most disparate sites (upstream vs. downstream) within a

drainage were consistently lower than the average of intra-drainage values. Higher degrees of structure detected within the Mississippi drainage however, may be influenced by the much larger distances between sites. This may suggest that IBD is more relevant is much larger drainage complexes such as the Mississippi drainage, although this should be further explored. Additionally, population genetic variations across both *P. riddelli* and *F. askewi* reflected patterns of differentiation possibly associated with factors such as dam barriers, local environmental shifts, or ecological interactions.

-*Pleurobema riddellii*

When examined at two clusters, *P. riddellii* samples are split between the Mississippi drainage and Texas rivers (Neches and Sabine drainages), largely conforming with expectations given this represents the largest geographical separation between populations. At three clusters samples taken from the Ouachita River sites split off as a separate group, displaying a disproportionately high level of differentiation relative to samples found within the same drainage system. This pattern was consistent across both methods of analysis; within the PCA Ouachita samples were separated from all others along PC II while maintaining an intermediate position along PC I between the two larger clusters. The distinctiveness of Ouachita and Little River samples are apparent given relatively high G_{ST} values as well as the pattern derived from clustering analyses which identified differentiation between within-drainage sites before between-drainage sites (Neches and Sabine). This pattern may indicate unique differentiation possibly resulting from local environmental and ecological interactions consistent with analyses of other species whose ranges overlap in the Ozark highland region (Elderkin et al., 2008). These differences may correspond to high levels of endemism within the surrounding tributaries

(Mayden, 1985; Vaughn et al., 1996; Crandall, 1998) and potentially associated host-specificity for local species or ecotypes (Riusech, 1998).

Four clusters resulted in a split between the Neches and Sabine drainages of East Texas, which as previously mentioned is interesting given the Ouachita populations split beforehand at k=3. This was, again, mirrored by our initial PCA findings as the two drainages appear as a single tight cluster in PC's I and II, only splitting along PC III. Limited divergence between these two basins is not surprising given the proximity and likely historical connection they shared during the last glacial maximum (Blum & Hattier-Womack, 2009; Blum et al., 2013) This pattern may be further exacerbated by the present geographical relationship between the Neches and Sabine systems- rather than independently draining into the Gulf of Mexico both systems terminate at the Sabine Lake embayment, potentially facilitating glochidia dispersal via host migration between the two basins granted sufficient fresh-water flow rates. However, results from both the larger *P. riddellii* assembly (Neches, Sabine, and Mississippi drainages) as well as the Texas-only assembly (Neches and Sabine drainages) show appreciable differentiation between these two drainages with limited evidence of recent mixing consistent with similar studies (Smith et al., 2021). This differentiation could be partially due to all Sabine samples coming from the upper reaches of the Sabine River (upstream of Toledo Bend dam), however could also be representative of limited secondary contact post isolation.

At five clusters the Neches group, representing the largest sample collection within the assembly, began to show a gradient of intra-drainage substructure among the three sampled waterways: the Angelina River, the Neches River, and the LNVA canal

system. While no significant pattern emerged between the Angelina and Neches Rivers, the LNVA canal did show a higher degree of differentiation relative to the others. This differentiation appears even more pronounced when looking at the Texas-only assembly. These results may come as a result of the unique environmental conditions created by human activity. Though such high-resolution differences within the drainage are likely not indicative of major isolation between populations as reflected in G_{ST} values largely consistent with other pairwise comparisons within the Neches. One canal site, however, did demonstrate significantly higher values across all comparisons (NCNL01; Table 3). The differentiation seen in this site and unique habitat may warrant future sampling and analysis. At larger k's the model begins to break down, showing more less significant sub-structure within the Neches sample group.

Fusconaia askewi

The assembly for *F. askewi* only represented the Neches and Sabine drainages, however samples were obtained from both the upper- and lower-Sabine River (defined by being up or downstream of Toledo Bend Dam respectfully). This was reflected in the initial PCA, displaying three clusters representing the Neches, upper Sabine, and lower Sabine sample groups. The Neches cluster, represented by two sample sites (henceforth referred to as upper and lower Neches), showed more variability between sites that either of the two Sabine clusters with the lower Neches site falling more closely to the Sabine groups along PC I.

Entropy results revealed an interesting resolution at two clusters for this taxon, splitting the lower-Sabine group out from the single cluster of the Neches and upper-Sabine groups. This pattern is also reflected in the G_{ST} values with lower- and upper-

Sabine comparisons showing higher values on average than comparisons across drainages (Neches vs. Sabine) or comparisons within drainages (Neches and upper-Sabine). Given that the genetic differentiation of this site outweighs the historical divergence between drainages, significant differentiation in lower-Sabine populations is likely associated with local environmental differences downstream of the Toledo Bend dam as well as the dam's role as a physical barrier to gene flow between the upper and lower reaches. Although little evidence has been found that displays significant impoundment-based differences in long term sediment transport, deposition, and channel morphology (Phillips, 2003) research has shown differences in factors such as species richness and abundance, turbidity, temperature, and corresponding life strategies of local species dependent on proximity and position relative to the Toledo Bend impoundment (Randklev et al., 2015; Schaefer et al., 2011). Slight admixture with the lower-Sabine cluster can also be found in the lower-Neches population, further indicating a historical connection and potential contemporary, albeit limited, gene flow between the lower reaches of the two drainages.

At three clusters the sampled populations are resolved into the clusters found in the initial PCA: the Neches, upper-Sabine, and lower-Sabine. This being more indicative of expectations given allopatric drainage divergence and intra-drainage proximity. At four clusters and beyond the model again begins to break down, showing non-significant levels of sub-structure across the upper-Sabine populations.

-*P. amphichaenus*

Results for *P. amphichaenus* samples reflected a clear separation between populations of the Sabine and Neches evident in both PCA (PC I) and Entropy (k=2)

analyses. These results remain consistent with similar studies (Smith et al., 2021) as well as previous analyses in this report. Again, this level of divergence between drainages is not surprising given the disparate sampling locations particularly the Sabine individuals all coming from sites in the upper reaches of the Sabine River. This collection of analyses again demonstrates evidence for historical divergence between basins with all species here showing similar levels of G_{ST} across Neches and Sabine comparisons.

V. CONCLUSIONS

This study analyzed the population genetic structure of three Unionid mussel species across two drainages of East Texas, including an expanded sample range for the primary species, *P. riddellii*. While genetic structure broadly comported with a model of isolation by distance and historical drainage connectivity, particular clusters within the Ouachita (*P. riddellii*) and lower-Sabine (*F. askewi*) rivers expressed unique signatures of differentiation. Differences within the Ouachita sample region may be due to environmental and ecological factors that correspond to the region's high degree of endemism and role as a glacial refugium, whereas individuals from the lower-Sabine may reflect the impact from the Toledo Bend impoundment serving as a direct barrier to gene-flow as well as its resulting perturbations to the biotic and abiotic environment downstream. Additionally, *P. riddellii* samples collected from the Neches drainage display a pattern of sub-structure at higher levels of k that may warrant further investigation. This is particularly noticeable when examining samples from the LNVA canal system relative to those collected further upstream. Across species, assemblies showed a general congruence of divergence between the Neches and Sabine drainages of East Texas, however it is possible this is influenced by the limited sampling distribution in the Sabine. The results reported here support the hypothesis of appreciable differentiation between drainages, however does not comport with the isolation by distance within the Neches or Sabine drainages. While isolation by distance most likely plays a role in the disparate Ouachita and Little River populations, this is likely also compounded by local environmental differences and species diversity. These analyses provide a useful model to gauge the factors and processes that influence patterns of

Unionid structure and divergence that should only be amplified by more comprehensive sampling. Further sampling and analyses across the uniquely differentiated regions identified here may provide a more concrete picture of population structure within and across Unionid species, as well as grant more insight into the specific environmental and ecological variables that govern the formation of population units.

TABLES

Table 1: Assembly collection size and SNP count.

Assembly	Species	N	# SNPs
Total	*P. riddellii, F. askewi, P. amphichaenus, L. fragilis, C. pustulosa*	352	3,621
Total PLRI	*P. riddellii*	146	14,928
TX PLRI	*P. riddellii*	130	14,955
FUAS	*F. askewi*	96	26,755
POAM	*P. amphichaenus*	28	21,022

Table 2: Total sampling effort for *P. riddellii*. Each sampling site includes its respective drainage, river, coordinates, and number of individuals collected. The Upper-Sabine River is defined as being upstream of Toledo Bend Dam.

Drainage	River	Site Code	Latitude	Longitude	N
Neches	Angelina River	ANG01	31.45797833	-94.7288054	7
Neches	Neches River	NECH01	31.19669	-94.85869	1
Neches	Neches River	NECH02	31.033791	-94.2995	27
Neches	Neches River	NECH03	30.59974	-94.0799	1
Neches	Neches River	NECH04	30.25476503	-94.10625369	6
Neches	Neches River	NECH05	30.255805	-94.170894	3
Neches	Neches River	NECH06	30.24173363	-94.11965612	9
Neches	LNVA canal	NCNL01	30.110777	-94.236456	2
Neches	LNVA canal	NCNL02	30.064019	-94.244214	19
Neches	LNVA canal	NCNL03	29.931548	-94.229618	19
Sabine	Upper-Sabine River	USAB02	32.529667	-94.959054	19
Sabine	Upper-Sabine River	USAB03	32.49685	-94.92622	2
Sabine	Upper-Sabine River	USAB04	32.45474	-94.891181	7
Sabine	Upper-Sabine River	USAB05	32.458218	-94.881588	2
Sabine	Upper-Sabine River	USAB06	32.46222	-94.845864	2
Sabine	Upper-Sabine River	USAB07	32.408538	-94.719713	2
Sabine	Upper-Sabine River	USAB08	32.411751	-94.71389	1
Mississippi	Big Cypress Bayou	BCB01	32.756632	-94.35803	1
Mississippi	Little River	LITT01	33.940604	-94.811604	11
Mississippi	Little River	LITT02	33.949177	-94.564193	1
Mississippi	Ouachita River	OUA01	33.62299	-92.83253	4

Table 3: Pairwise G_{ST} estimates for *P. riddellii* sample sites.

	ANG01	NECH02	NECH04	NECH05	NECH06	NCNL01	NCNL02	NCNL03	USAB02	USAB03	USAB04	USAB05	USAB06	USAB07	LITT01	OUA01
ANG01	0															
NECH02	0.0137	0														
NECH04	0.024	0.0159	0													
NECH05	0.0349	0.0272	0.0369	0												
NECH06	0.0199	0.0115	0.0215	0.0322	0											
NCNL01	0.0511	0.0432	0.0535	0.0655	0.0491	0										
NCNL02	0.0158	0.0078	0.0179	0.0278	0.0131	0.0446	0									
NCNL03	0.0165	0.0092	0.0187	0.0287	0.0142	0.045	0.0087	0								
USAB02	0.0202	0.0122	0.0223	0.033	0.0176	0.0491	0.014	0.0149	0							
USAB03	0.0561	0.0469	0.0582	0.0704	0.053	0.0861	0.049	0.05	0.0426	0						
USAB04	0.0269	0.019	0.0289	0.0398	0.0241	0.056	0.0204	0.0216	0.0147	0.0497	0					
USAB05	0.0553	0.0467	0.057	0.0699	0.0524	0.0851	0.0483	0.0495	0.0433	0.0794	0.0504	0				
USAB06	0.0563	0.0477	0.0583	0.0693	0.0533	0.0879	0.0492	0.0507	0.0431	0.0815	0.0501	0.0815	0			
USAB07	0.056	0.0473	0.058	0.0706	0.0534	0.0854	0.0489	0.05	0.0437	0.0806	0.0506	0.0795	0.0807	0		
LIT01	0.1444	0.1355	0.1467	0.1579	0.1406	0.1791	0.1363	0.1355	0.1319	0.1739	0.14	0.1722	0.1715	0.1718	0	
OUA01	0.0885	0.0796	0.0901	0.1006	0.0846	0.1203	0.0804	0.0809	0.079	0.1181	0.086	0.1152	0.1163	0.1169	0.1098	0

Table 4: Total sampling effort for *F. askewi.* Each sampling site includes its respective drainage, river, coordinates, and number of individuals collected.

Drainage	River	Site-code	Latitude	Longitude	N
Neches	Neches River	NECH02	31.033791	-94.2995	13
Neches	Neches River	NECH06	30.24173363	-94.11965612	3
Sabine	Upper-Sabine River	USAB01	32.62986	-95.35719	25
Sabine	Upper-Sabine River	USAB02	32.529667	-94.959054	17
Sabine	Upper-Sabine River	USAB06	32.46222	-94.845864	19
Sabine	Upper-Sabine River	USAB07	32.408538	-94.719713	2
Sabine	Lower-Sabine River	LSAB01	30.786391	-93.589476	17

Table 5: Pairwise G_{ST} estimates for *F. askewi* sample sites.

	NECH02	NECH06	USAB01	USAB02	USAB06	USAB07	LSAB01
NECH02	0						
NECH06	0.0427	0					
USAB01	0.0207	0.0438	0				
USAB02	0.0211	0.0442	0.0098	0			
USAB06	0.0213	0.044	0.0091	0.0098	0		
USAB07	0.0574	0.0816	0.0447	0.0464	0.0453	0	
LSAB01	0.0542	0.0609	0.0417	0.0414	0.0405	0.0809	0

Table 6: Total sampling effort for *P. amphichaenus.* Each sampling site include its respective drainage, river, coordinates, and number of individuals.

Drainage	River	Site-code	Latitude	Longitude	N
Neches	Neches River	NECH04	30.25476503	-94.10625369	20
Sabine	Upper-Sabine River	USAB08	32.411751	-94.71389	1
Sabine	Upper-Sabine River	USAB09	32.419294	-94.704589	1
Sabine	Upper-Sabine River	USAB10	32.377073	-94.466456	4
Sabine	Upper-Sabine River	USAB11	32.3743663	-94.4636498	1
Sabine	Upper-Sabine River	USAB12	32.213892	-94.22052	1

Table 7: Pairwise G_{ST} estimate between *P. amphichaenus* sample sites.

	NECH04	USAB10
NECH04	0	
USAB10	0.0429	0

FIGURES

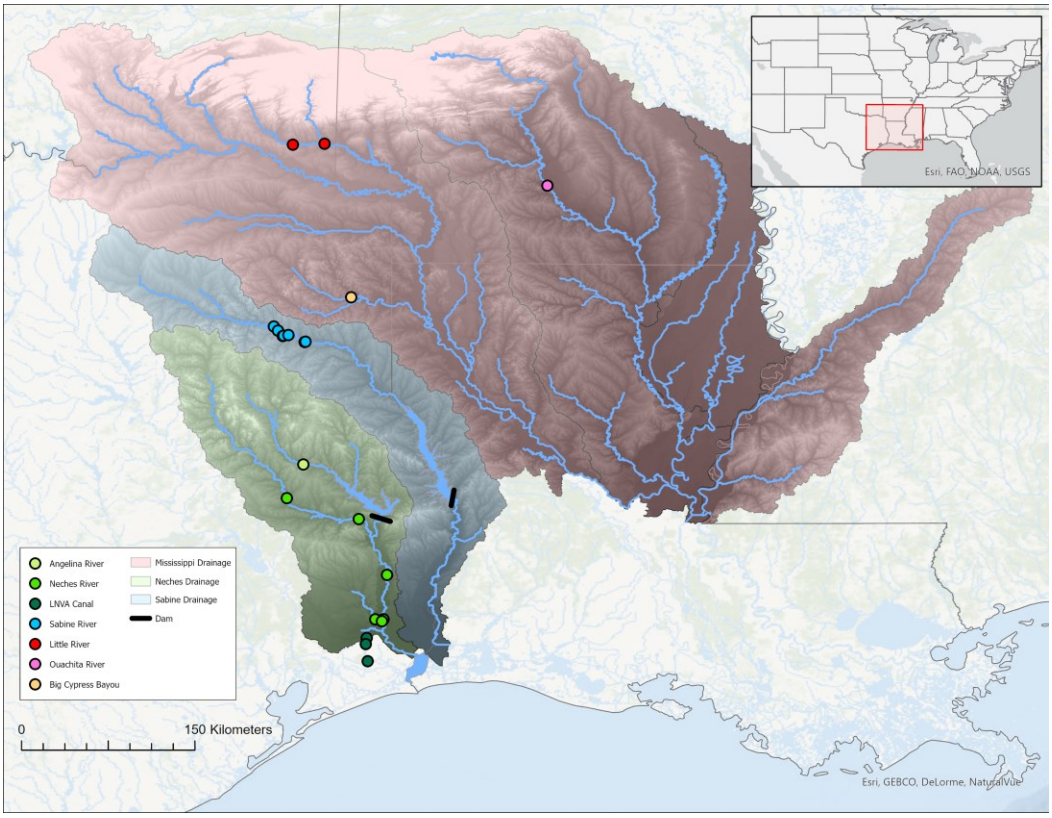

Figure 1: Map of sampling locations for *P. riddellii.* Points represent sampled river: Sabine R. (blue), Angelina R. (light green), Neches R. (green), LNVA canal (dark green), Big Cypress Bayou (orange), Little R. (red), and Ouachita R. (pink). Shading represents drainage basin: Neches (green), Sabine (blue), and Mississippi (red). Dark lines represent dams for Toledo Bend and Sam Rayburn Reservoirs.

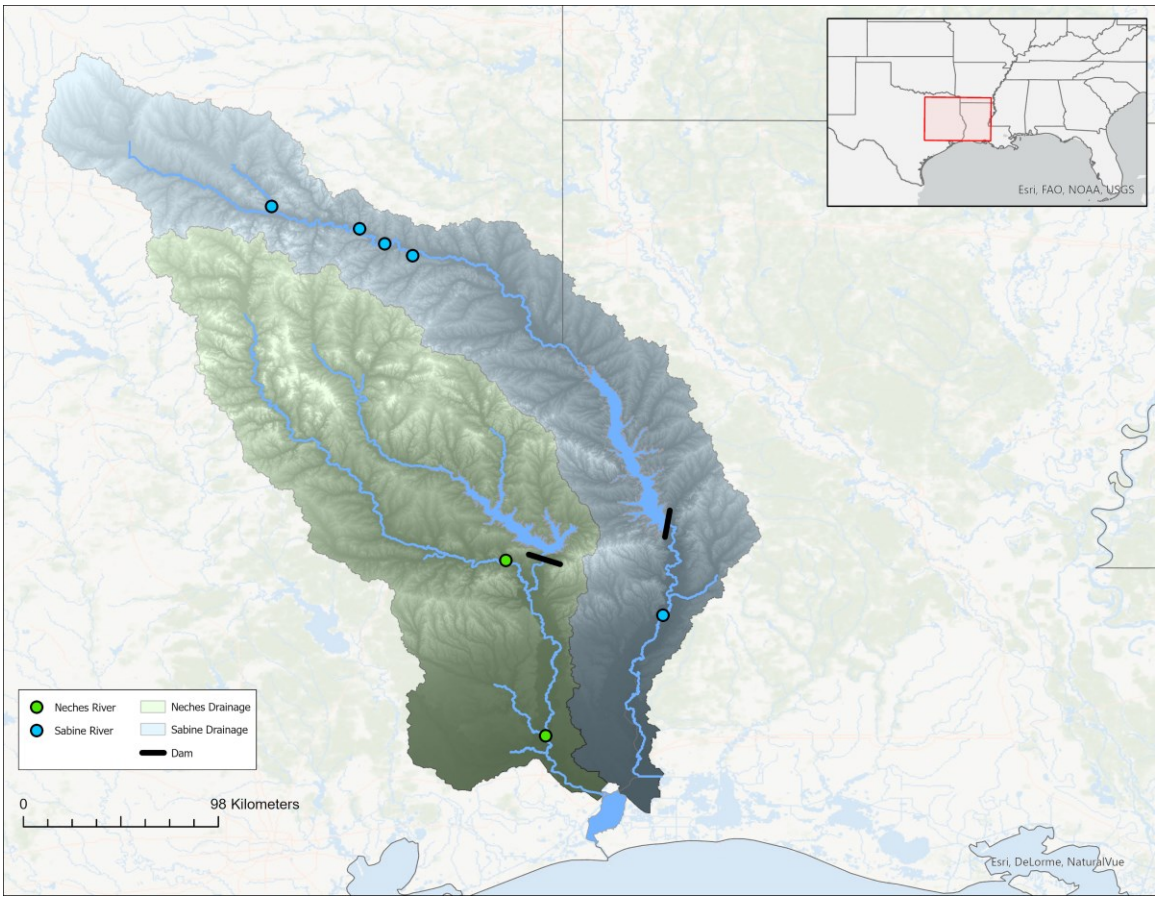

Figure 2: Map of sampling locations for *F. askewi*. Points represent sampled river: Sabine R. (blue) and Neches R. (green). Shading represents drainage basin: Neches (green) and Sabine (blue). Dark lines represent dams for Toledo Bend and Sam Rayburn Reservoirs.

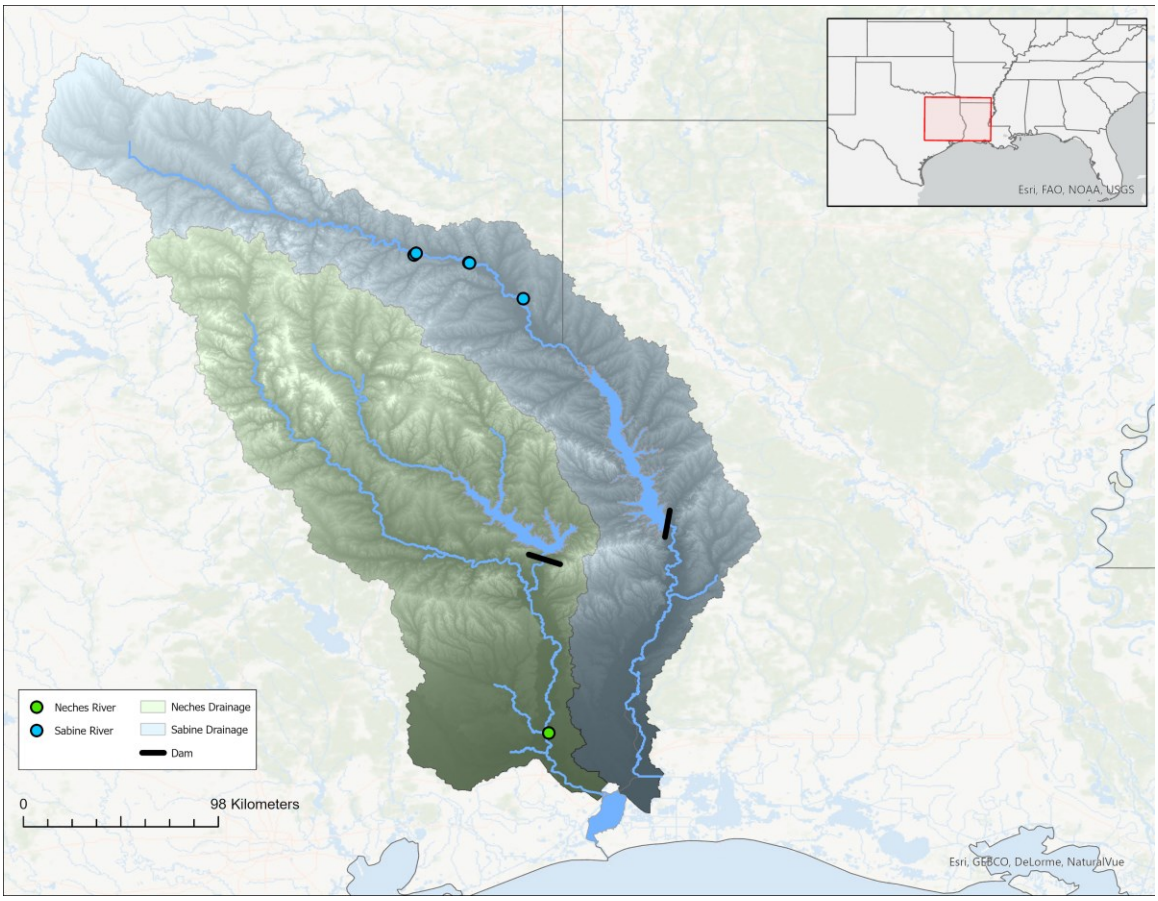

Figure 3: Map of sampling locations for *P. amphichaenus*. Points represent sampled river: Sabine R. (blue) and Neches R. (green). Shading represents drainage basin: Neches (green) and Sabine (blue). Dark lines represent dams for Toledo Bend and Sam Rayburn Reservoirs.

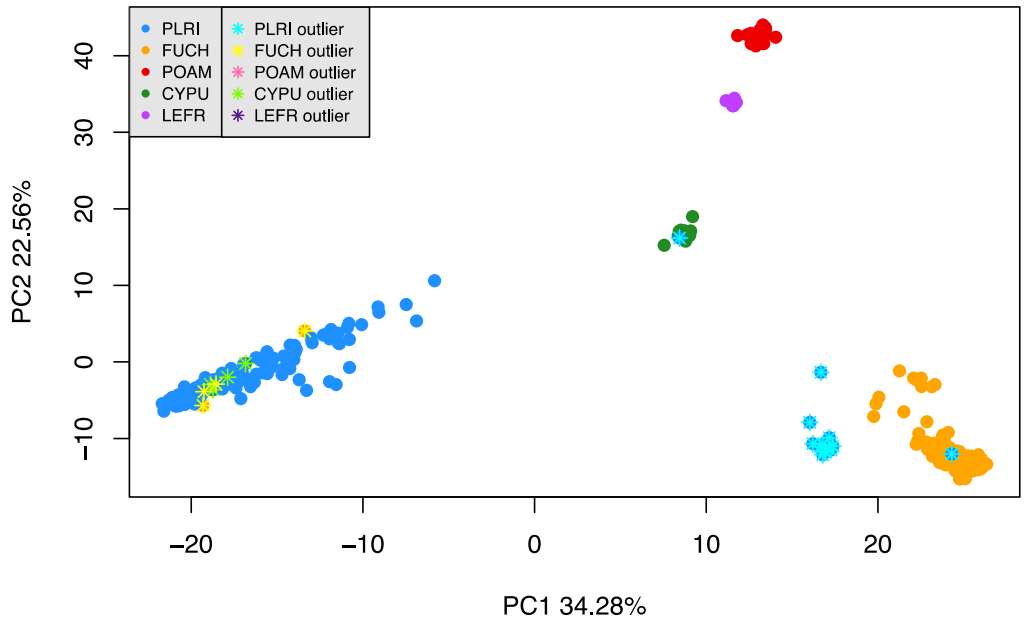

Figure 4: PCA of genotype data across all individuals and species. PC I explains approximately 34.28% of the variation, and PC II explains approximately 22.56% of the variation. Color corresponds to field ID's: *P. riddellii* (blue), *F. askewi* (orange), *P. amphichaenus* (red), *C. pustulosa* (green), *L. fragilis* (purple). Stars and lighter colors indicate individuals who do cluster with the species they were identified as, and likely represent misidentifications in the field.

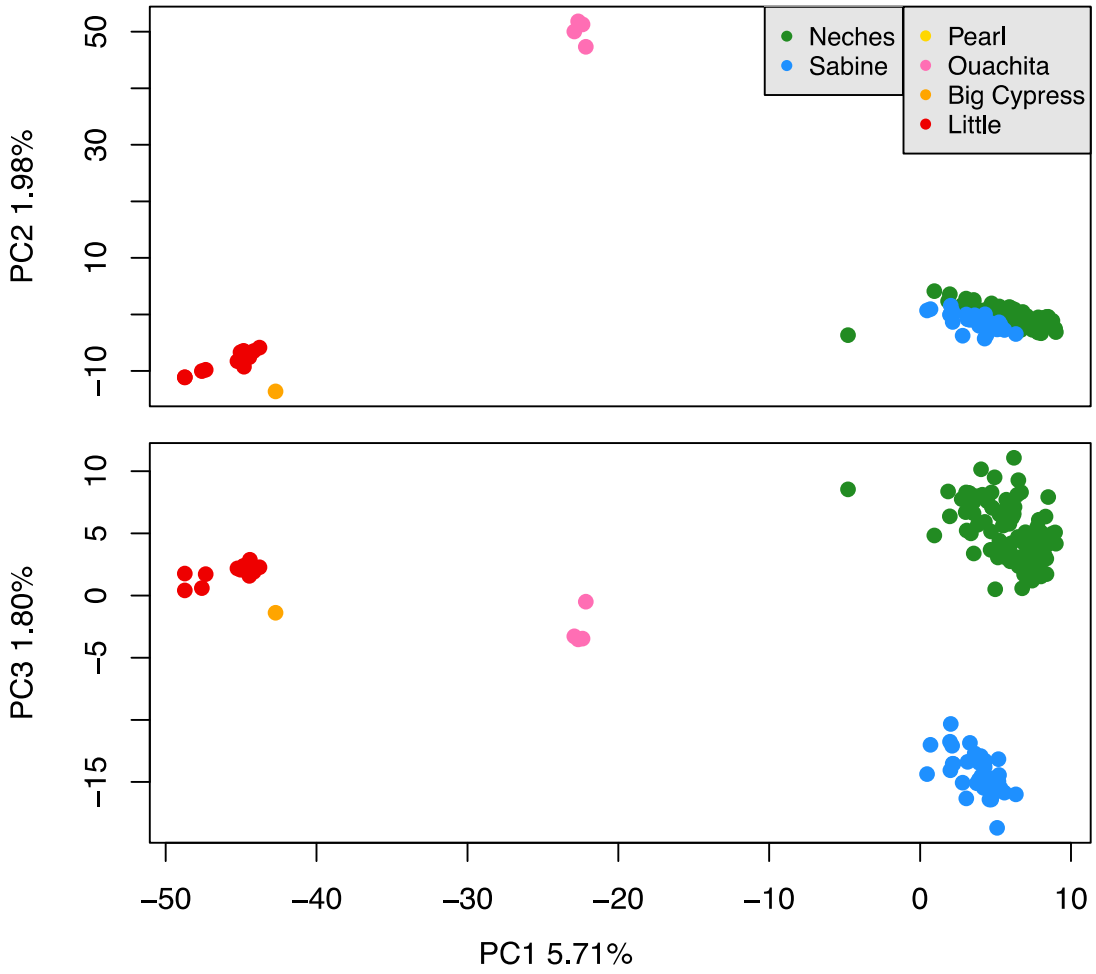

Figure 5: PCA of genotype likelihoods for the "total" *P. riddellii* assembly. PCs I, II, and III explain approximately 5.75%, 1.97%, and 1.79% of the variation respectively. Point colors represent sample locations: Neches drainage (green), Sabine R. (blue), Ouachita R. (pink), Big Cypress Bayou (orange), and Little R. (red).

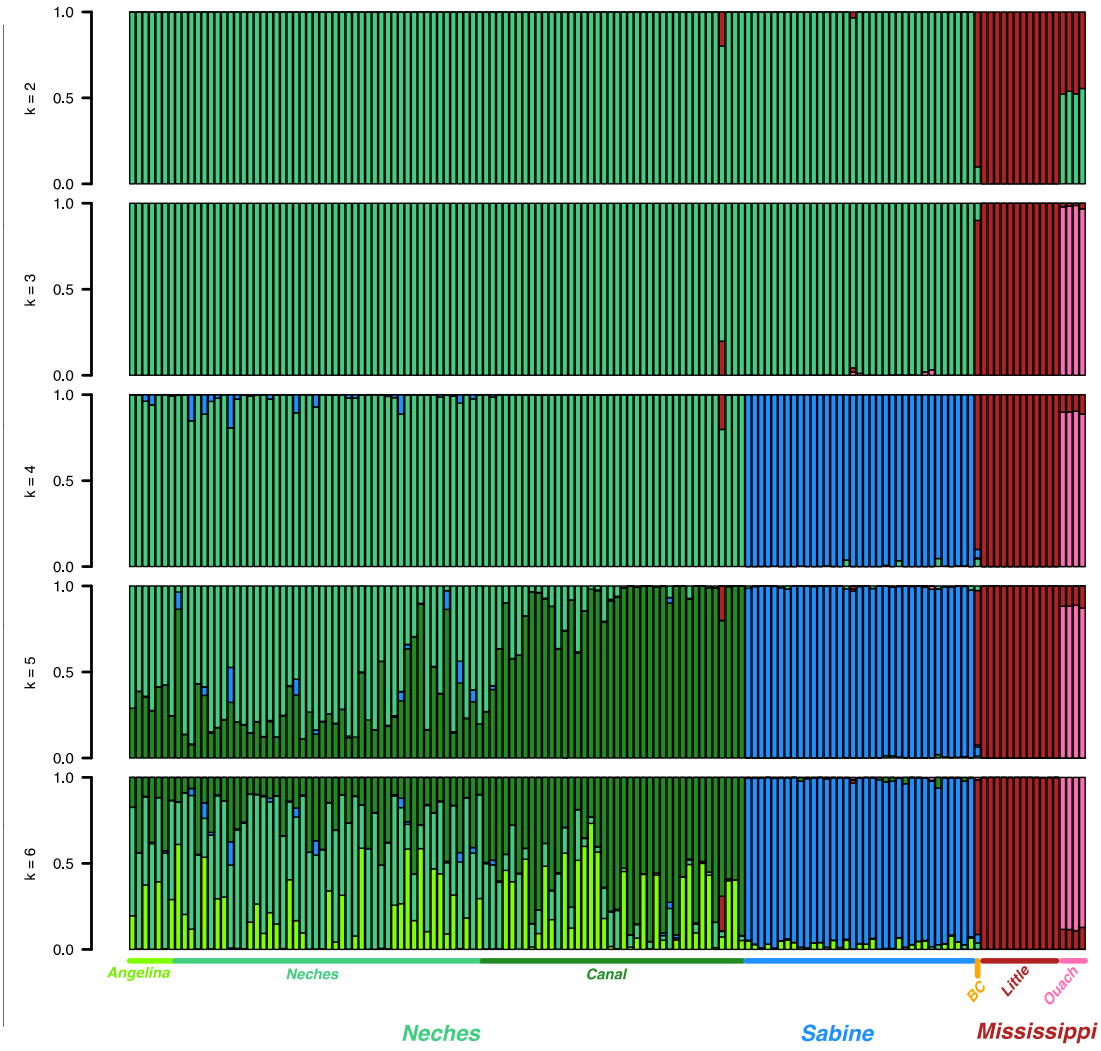

Figure 6: Entropy admixture plots of k = 2, 3, 4, 5, and 6 for the "total" *P. riddellii* assembly. Individuals are arranged from most upstream to most downstream (left to right) in each respective drainage. Labeling on the x axis includes all sampled rivers including the Angelina, Neches, LNVA canal (Canal), Sabine, Big Cypress Bayou (BC), Little, and Ouachita.

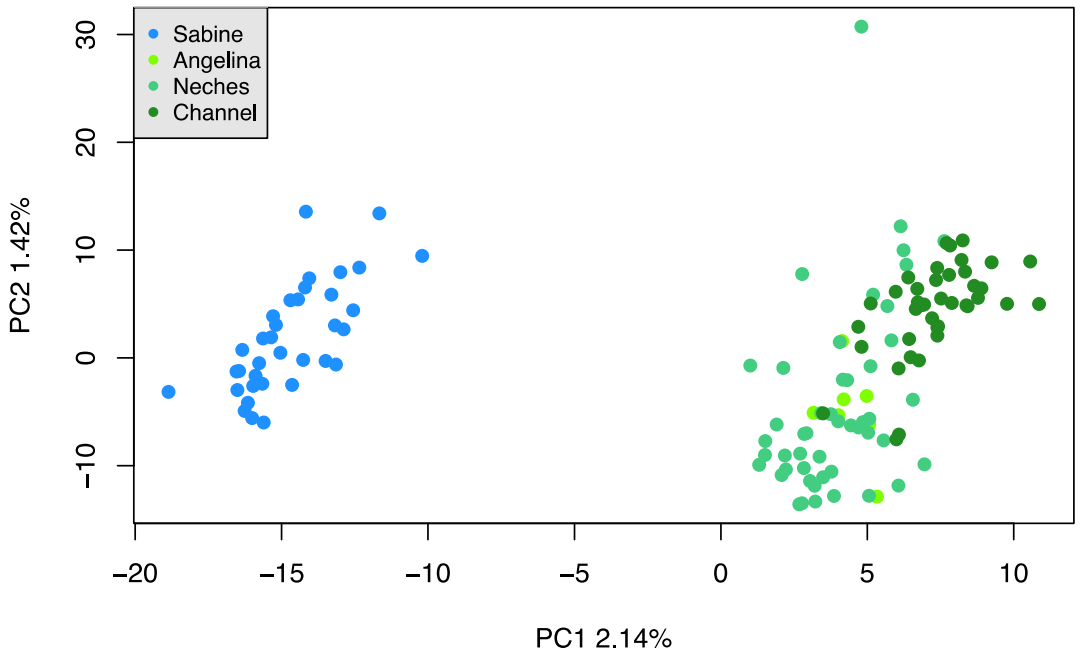

Figure 7: PCA of genotype likelihoods for the "Texas" *P. riddellii* assembly. PCs I and II explain approximately 2.14% and 1.42% of the variation respectively. Colors represent sample location: Sabine R. (blue), Angelina R. (light green), Neches R. (green), and LNVA canal (dark green).

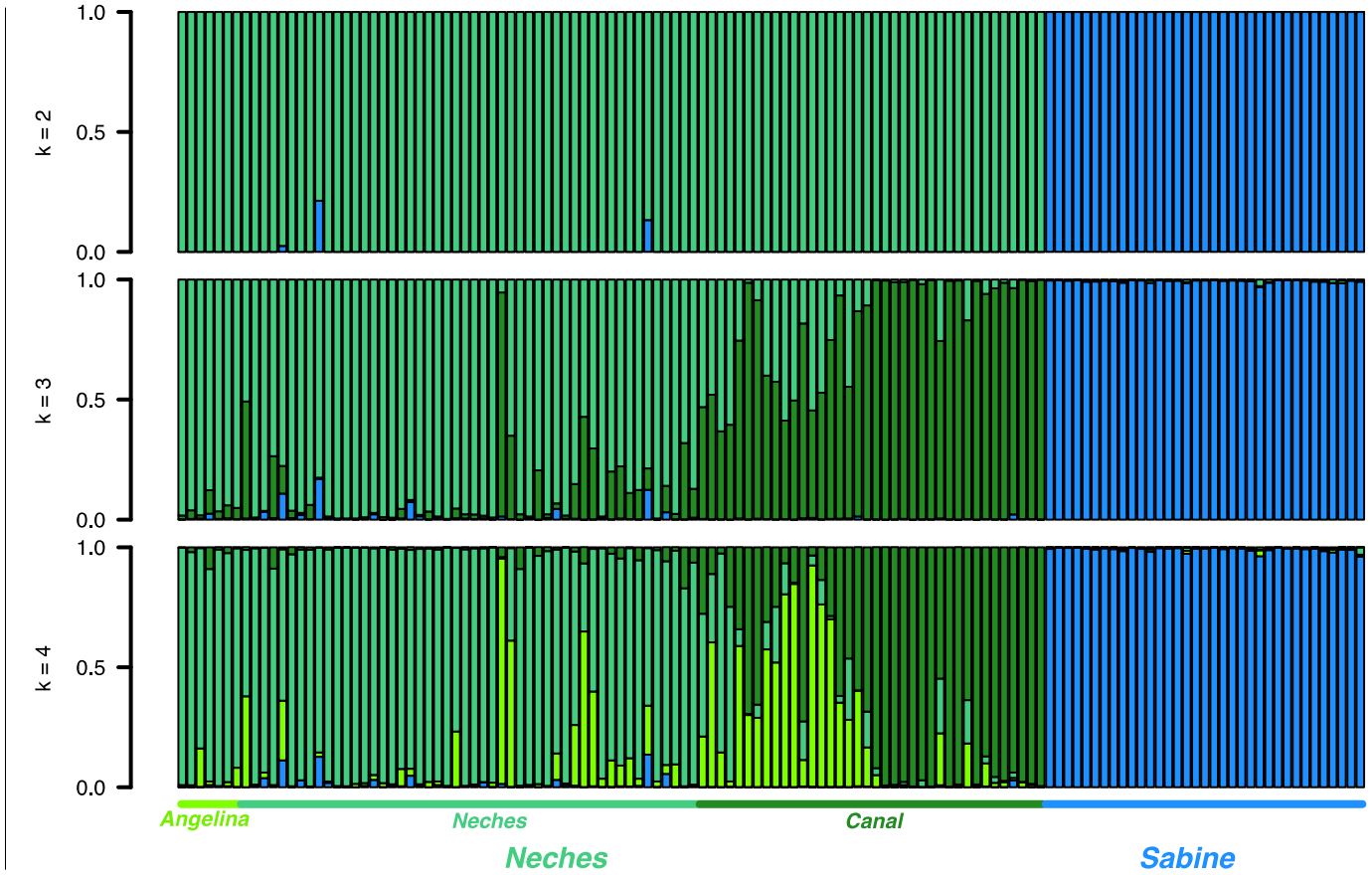

Figure 8: Entropy admixture plots of k=2, 3, and 4 for the "Texas" *P. riddellii* assembly. Individuals are arranged from most upstream to most downstream (left to right) for respective drainages (Neches and Sabine).

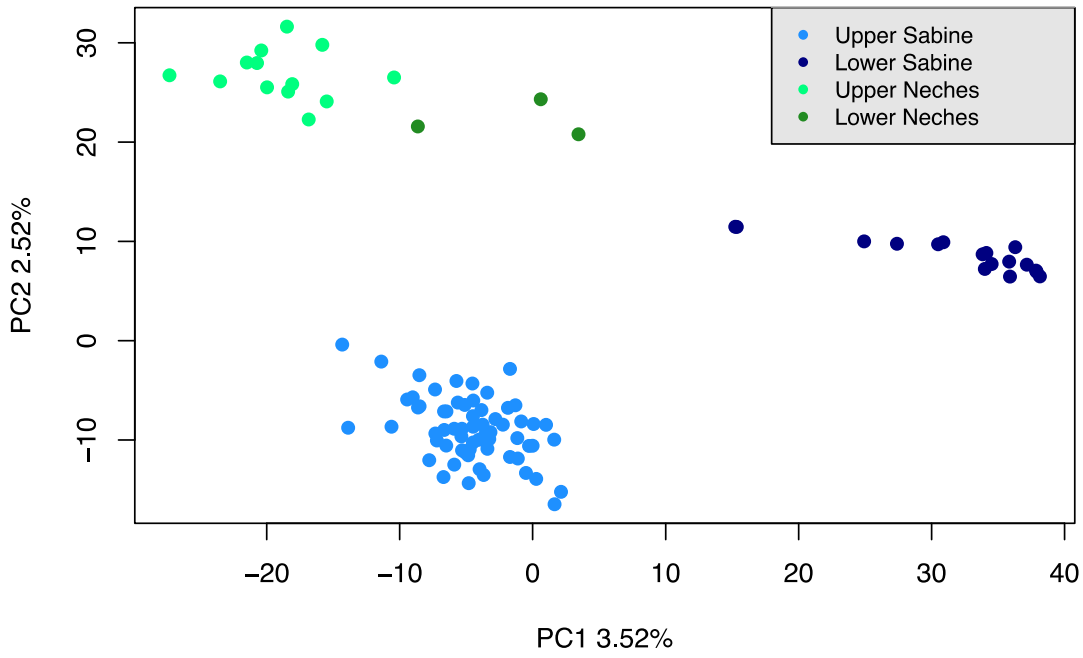

Figure 9: PCA of genotype likelihoods for the *F. askewi* assembly. PCs I and II explain approximately 3.52% and 2.52% of the total variation, respectively. Colors represent sample locations: upper Neches (light green), Lower Neches (dark green), Upper Sabine (light blue), and lower Sabine R. (dark blue). Upper and lower Sabine locations are separated by the Toledo Bend impoundment.

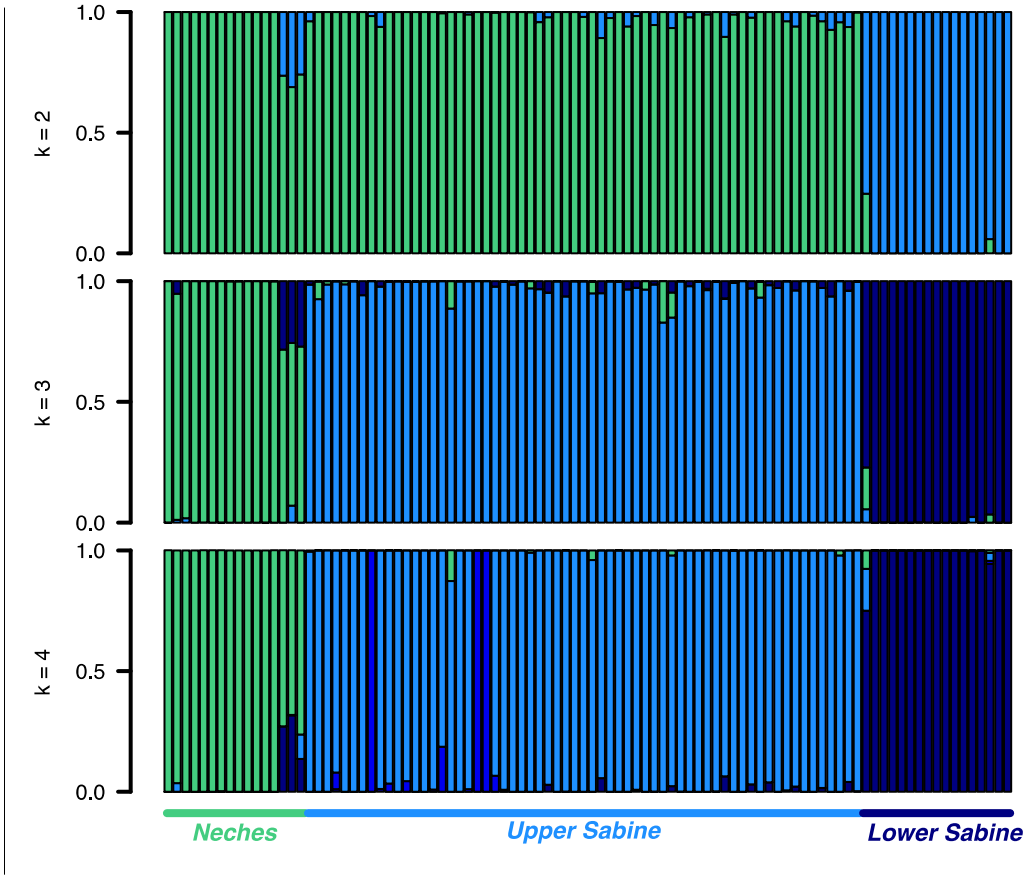

Figure 10: Entropy admixture plots of k=2, 3, and 4 for the *F. askewi* assembly. Individuals are arranged from most upstream to most downstream within each respective drainage (Neches and Upper and Lower Sabine).

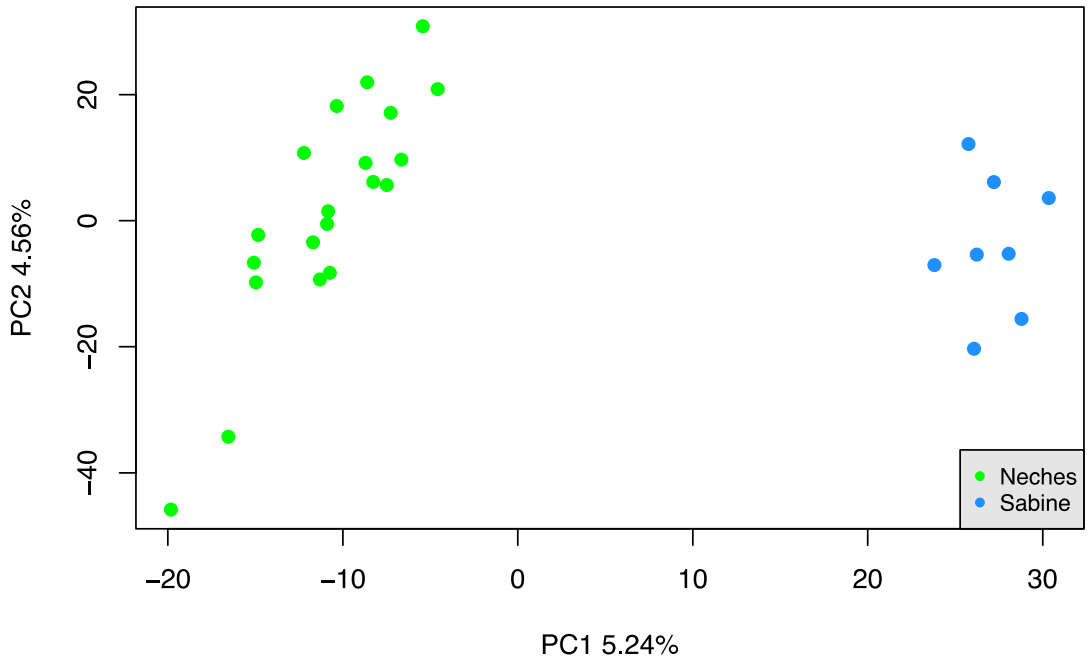

Figure 11: PCA of genotype likelihoods for the *P. amphichaenus* assembly. PCs I and II explain approximately 5.24% and 4.56% of the variation respectively. Colors represent sample drainage: Neches (green) and Sabine (blue).

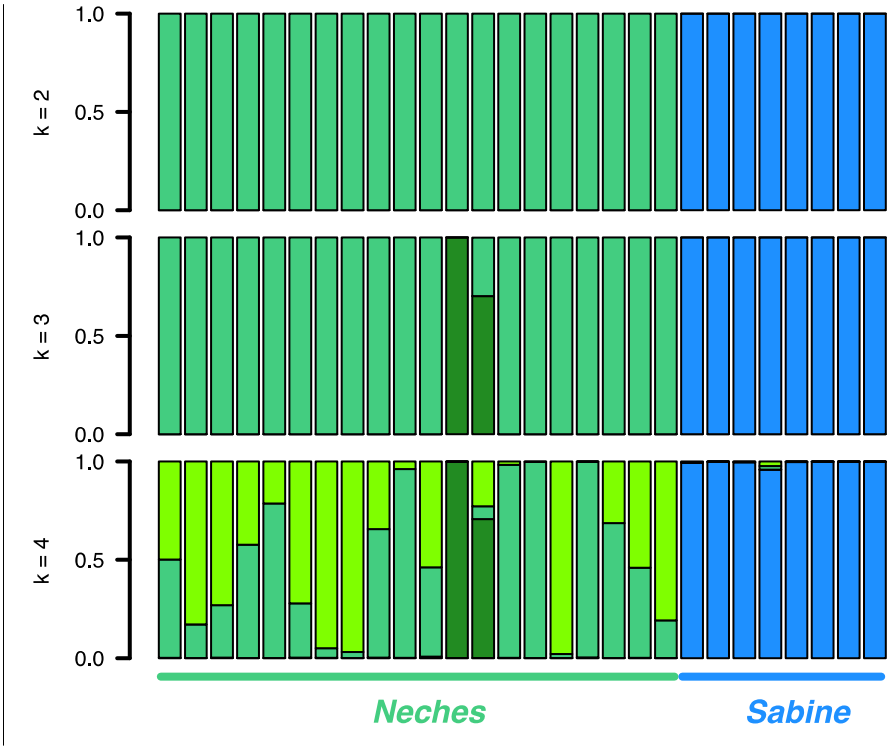

Figure 12: Entropy admixture plots of k=2, 3, and 4 for the *P. amphichaenus* assembly. Individuals are arranged from most upstream to most downstream (left to right) for each respective drainage (Neches and Sabine).

LITERATURE CITED

Archambault, J.M., Cope, W.G. and Kwak, T.J. 2014. Survival and behaviour of juvenile unionid mussels exposed to thermal stress and dewatering in the presence of a sediment temperature gradient. Freshwater Biology, 59: 601-613.

Barnhart, C.M., Haag, W.R., and Roston, W.N. 2008. Adaptations to host infection and larval parasitism in Unionoida. Freshwater Science, 27: 370-394.

Bolnick, D.I. and Fitzpatrick, B.M. 2007. Sympatric Speciation: Models and Empirical Evidence. Annual Review of Ecology, Evolution, and Systematics, 38: 459-487.

Burlakova, L.E., Campbell, D., Karatayev, A.Y. and Barclay, D. 2012. Distribution, genetic analysis and conservation priorities for rare Texas freshwater molluscs in the genera Fusconaia and Pleurobema (Bivalvia: Unionidae). Aquatic Biosystems, 8: 12.

Bush, G.L. 1969. Sympatric Host Race Formation and Speciation in Frugivorous Flies of the Genus Rhagoletis (Diptera, Tephritidae). Evolution, 23: 237-251.

Blum, M. D., & Hattier-Womack, J. 2009. Climate change, sea-level change, and fluvial sediment supply to deepwater systems. SEPM Spec P 92: 15–39.

Blum, M., Martin, J., Milliken, K., & Garvin, M. 2013. Paleovalley systems: Insights from Quaternary analogs and experiments. Earth Science Reviews, 116: 128–169.

Cañedo-Argüelles, M., Kefford, B. J., Piscart, C., Prat, N., Schäfer, R. B., & Schulz, C.-J. 2013. Salinisation of rivers: An urgent ecological issue. Environmental Pollution, 173: 157–167.

Crandall, K. 1998. Conservation phylogenetics of Ozark crayfishes: Assigning priorities for aquatic habitat protection. Biological Conservation I, 84: 107-117.

Dudgeon, D., Arthington, A.H., Gessner, M.O., Kawabata, Z.-I., Knowler, D.J., Lévêque, C., Naiman, R.J., Prieur-Richard, A.-H., Soto, D., Stiassny, M.L.J. and Sullivan, C.A. 2006. Freshwater biodiversity: importance, threats, status and conservation challenges. Biological Reviews, 81: 163-182.

Elderkin, C.L., Christian, A.D., Metcalfe-Smith, J.L. and Berg, D.J. 2008. Population genetics and phylogeography of freshwater mussels in North America, Elliptio dilatata and Actinonaias ligamentina(Bivalvia: Unionidae). Molecular Ecology, 17: 2149-2163.

Ewers, R.M. and Didham, R.K. 2006. Confounding factors in the detection of species responses to habitat fragmentation. Biological Reviews, 81: 117-142.

Falush, D., Stephens, M., & Pritchard, J. K. 2003. Inference of population structure using multilocus genotype data: Linked loci and correlated allele frequencies. Genetics, 164: 1567–1587.

Ferguson, C.D., Blum, M.J., Raymer, M.L., Eackles, M.S., and Krane, D.E. 2013. Population structure, multiple paternity, and long-distance transport of spermatozoa in the freshwater mussel Lampsilis cardium (Bivalvia: Unionidae). Freshwater Science, 32: 267-282.

Ford, D.F., Plants-Paris, E.D. and Ford, N.B. 2020. Comparison of Louisiana Pigtoe (Pleurobema riddellii, Mollusca, Unionidae) growth at three different locations in the Neches River Basin of East Texas. Hydrobiologia, 847: 2021-2033.

Fu, L., Niu, B., Zhu, Z., Wu, S., & Li, W. 2012. CD-HIT: Accelerated for clustering the next-generation sequencing data. Bioinformatics, 28: 3150–3152.

Funk, W. C., McKay, J. K., Hohenlohe, P. A., & Allendorf, F. W. 2012. Harnessing genomics for delineating conservation units. Trends in Ecology & Evolution, 27: 489–496.

Gargominy, O., Herbert, D.G., Hershler, R., Perez, K.E., Roth, B., Seddon, M., Strong, E.E. and Thompson, F.G. 2004. The Global Decline of Nonmarine Mollusks. BioScience, 54: 321-330.

Gompert, Z., Lucas, L.K., Buerkle, C.A., Forister, M.L., Fordyce, J.A. and Nice, C.C. 2014. Admixture and the organization of genetic diversity in a butterfly species complex revealed through common and rare genetic variants. Molecular Ecology, 23: 4555-4573.

Gompert, Z., Lucas, L.K., Nice, C.C., Fordyce, J.A., Forister, M.L. and Buerkle, C.A. 2012. Genomic Regions with a History of Divergent Selection Affect Fitness of Hybrids Between Two Butterfly Species. Evolution, 66: 2167-2181.

Graf, D.L. and Cummings, K.S. 2007. Review of the systematics and global diversity of freshwater mussel species (Bivalvia: Unionoida). Journal of Molluscan Studies, 73: 291-314.

Hanski, I., Pakkala, T., Kuussaari, M. and Lei, G. 1995. Metapopulation Persistence of an Endangered Butterfly in a Fragmented Landscape. Oikos, 72: 21-28.

Howells, R.G., Randklev, C.R., and Ford, N.B. 2017. Accuracy of freshwater Mussel Identification: Results from a Study in Texas. American Conchologist 45: 9-17.

Irmscher, P. and Vaughn, C.C. 2018. Effects of Juvenile Settling and Drift Rates on Freshwater Mussel Dispersal. The American Midland Naturalist, 180: 258-272, 215.

Li H. (2011). A statistical framework for SNP calling, mutation discovery, association mapping and population genetical parameter estimation from sequencing data. Bioinformatics, 27(21): 2987-93.

Li, H. and Durbin, R. 2009. Fast and accurate short read alignment with Burrows–Wheeler transform. Bioinformatics, 25: 1754-1760.

Li, W. and Godzik, A. 2006. Cd-hit: a fast program for clustering and comparing large sets of protein or nucleotide sequences. Bioinformatics, 22: 1658-1659.

Lydeard, C., Cowie, R.H., Ponder, W.F., Bogan, A.E., Bouchet, P., Clark, S.A., Cummings, K.S., Frest, T.J., Gargominy, O., Herbert, D.G. and Hershler, R., 2004. The global decline of nonmarine mollusks. BioScience, 54(4): 321-330.

Mandeville, E.G., Parchman, T.L., McDonald, D.B. and Buerkle, C.A. 2015. Highly variable reproductive isolation among pairs of Catostomus species. Molecular Ecology, 24: 1856-1872.

Mayden, R. L. (1985). Biogeography of Ouachita Highland Fishes. The Southwestern Naturalist, 30(2): 195–211.

Meyer, M. and Kircher, M. 2010. Illumina Sequencing Library Preparation for Highly Multiplexed Target Capture and Sequencing. Cold Spring Harbor Protocols, 2010: pdb.prot5448.

Nei, M. 1987. Molecular evolutionary genetics. New York, NY: Columbia University Press.

Olson, P.J. and Vaughn, C.C. 2020. Population Genetics of a Common Freshwater Mussel, Amblema plicata, in a Southern U.S. River. Freshwater Mollusk Biology and Conservation, 23: 124-133, 110.

Parchman, T.L., Gompert, Z., Braun, M.J., Brumfield, R.T., McDonald, D.B., Uy, J.A.C., Zhang, G., Jarvis, E.D. 2012. Genome-wide association genetics of an adaptive trait in lodgepole pine. Molecular Ecology, 21: 2991-3005.

Phillips, J.D. 2003. Toledo Bend reservoir and geomorphic response in the lower Sabine River. River Res. Applic., 19: 137-159.

Philips, J. D., Slattery, M. C., & Musselman, Z. A. 2004. Dam-to-delta sediment inputs and storage in the lower Trinity River, Texas. Geomorphology, 62: 17–34.

Pritchard, J. K., Stephens, M., & Donnelly, P. 2000. Inference of population structure using multilocus genotype data. Genetics, 155: 945–959.

Puritz, J.B., Hollenbeck, C.M. and Gold, J.R. 2014. dDocent: a RADseq, variant-calling pipeline designed for population genomics of non-model organisms. PeerJ, 2: e431.

Purvis, A., Gittleman, J.L., Cowlishaw, G. and Mace, G.M. 2000. Predicting extinction risk in declining species. Proceedings of the Royal Society of London. Series B: Biological Sciences, 267: 1947-1952.

R Core Team 2021. R: A language and environment for statistical computing. R Foundation for Statistical Computing, Vienna, Austria.

Randklev, C. R., Lundeen, B. J., Skorupski, J., Kennedy, J. H., & Wolverton, S. 2011. Toledo bend relicensing project: Lower Sabine River mussel study. Sabine River Authority.

Randklev, C.R., Ford, N., Wolverton, S., Kennedy, J.H., Robertson, C., Mayes, K. and Ford, D. 2016. The influence of stream discontinuity and life history strategy on mussel community structure: a case study from the Sabine River, Texas. Hydrobiologia, 770(1): 173-191

Ricciardi, A., Neves, R.J. and Rasmussen, J.B. 1998. Impending extinctions of North American freshwater mussels (Unionoida) following the zebra mussel (Dreissena polymorpha) invasion. Journal of Animal Ecology, 67: 613-619.

Riley, S.P.D., Pollinger, J.P., Sauvajot, R.M., York, E.C., Bromley, C., Fuller, T.K. and Wayne, R.K. 2006. FAST-TRACK: A southern California freeway is a physical and social barrier to gene flow in carnivores. Molecular Ecology, 15: 1733-1741.

Riusech, F.A. and Barnhart, C.M. 1998. Host suitability and utilization in Venustaconcha ellipsiformis and Venustaconcha pleasii (Bivalvia: Unionidae) from the Ozark Plateaus. Proceedings of the Conservation, Captive Care, and Propagation of Freshwater Mussels Symposium: 83-91.

Schaefer, J.F., Duvernell, D.D. & Kreiser, B.R. 2011. Ecological and genetic assessment of spatial structure among replicate contact zones between two topminnow species. Evol Ecol, 25: 1145–1161.

Schlinger, B.A. and Buerkle, C.A. 2013. The genomic consequences of adaptive divergence and reproductive isolation between species of manakins. Molecular Ecology, 22: 3304-3317.

Schwalb, A.N., Cottenie, K., Poos, M.S. and Ackerman, J.D. 2011. Dispersal limitation of unionid mussels and implications for their conservation. Freshwater Biology, 56: 1509-1518.

Smith, C. H., Johnson, N. A., Robertson, C. R., Doyle, R. D., & Randklev, C. R. 2021. Establishing conservation units to promote recovery of two threatened freshwater mussel species (Bivalvia: Unionida: Potamilus). Ecology and Evolution, 11: 11102– 11122.

Sotola, VA, Ruppel, DS, Bonner, TH, Nice, CC, Martin, NH. 2018. Asymmetric introgression between fishes in the Red River basin of Texas is associated with variation in water quality. Ecol Evol, 9: 2083– 2095.

Spieth, P.T. 1974. Gene Flow and Genetic Differentiation. Genetics, 78: 961-965

Spieth, P.T. 1979. Environmental Heterogeneity: A Problem of Contradictory Selection Pressures, Gene Flow, and Local Polymorphism. The American Naturalist, 113: 247-260.

Steeves, T.E., Anderson, D.J., McNally, H., Kim, M.H. and Friesen, V.L. 2003. Phylogeography of Sula: the role of physical barriers to gene flow in the diversification of tropical seabirds. Journal of Avian Biology, 34: 217-223.

Strayer, D.L., Downing, J.A., Haag, W.R., King, T.L., Layzer, J.B., Newton, T.J. and Nichols, J.S. 2004. Changing Perspectives on Pearly Mussels, North America's Most Imperiled Animals. BioScience, 54: 429-439.

Strayer, D.L. 2008. Freshwater Mussel Ecology: A Multifactor Approach to Distribution and Abundance. Berkeley: University of California Press.

Templeton, A.R., Shaw, K., Routman, E. and Davis, S.K. 1990. The Genetic Consequences of Habitat Fragmentation. Annals of the Missouri Botanical Garden, 77: 13-27.

TPWD 2020. Threatened and endangered nongame species. Chapter 65. Wildlife subchapter G. Rule §65.175. Adopted rules. Texas Secretary of State.

Trizio, I., Crestanello, B., Galbusera, P., Wauters, L.A., Tosi, G., Matthysen, E. and Hauffe, H.C. 2005. Geographical distance and physical barriers shape the genetic structure of Eurasian red squirrels (Sciurus vulgaris) in the Italian Alps. Molecular Ecology, 14: 469-481.

Vannote, R.L., Minshall, G.W., Cummins, K.W., Sedell, J.R., & Cushing, C.E. 1980. The River Continuum Concept. Canadian Journal of Fisheries and Aquatic Sciences. 37(1): 130-137.

Vaughn, C. C., Mather, C. M., Pyron, M., Mehlhop, P., & Miller, E. K. 1996. The Current and Historical Mussel Fauna of the Kiamichi River, Oklahoma. The Southwestern Naturalist, 41(3), 325–328.

Webb, J.K., Brook, B.W. and Shine, R. 2002. What makes a species vulnerable to extinction? Comparative life-history traits of two sympatric snakes. Ecological Research, 17: 59-67.

Wellmeyer, J. L., Slattery, M. C., & Phillips, J. D.2005. Quantifying downstream impacts of impoundment on flow regime and channel planform, lower Trinity River, Texas. Geomorphology, 69, 1–13.

Williams, J.D., Warren Jr., M.L., Cummings, K.S., Harris, J.L. and Neves, R.J. 1993. Conservation Status of Freshwater Mussels of the United States and Canada. Fisheries, 18: 6-22.

Zalewski, A., Piertney, S.B., Zalewska, H. and Lambin, X. 2009. Landscape barriers reduce gene flow in an invasive carnivore: geographical and local genetic structure of American mink in Scotland. Molecular Ecology, 18: 1601-1615.